Originals

Experiments in Fluids 27 (1999) 473–483 © Springer-Verlag 1999

Considerations about the phase averaging method with application to ELDV and PIV measurements over pitching airfoils

P. Wernert, D. Favier

Abstract Some considerations about the principles of the phase averaging method, often used to decompose a measured signal into mean and fluctuating parts, are presented for periodic flow configurations involving natural and forced unsteadiness. The order of procedure to theoretically determine the number N of cycles required to perform a correct phase averaging decomposition is discussed and a practical criterion is proposed. The use of this criterion is first illustrated in the case of ELDV measurements in and outside the boundary-layer on an airfoil oscillating in pitch at moderate conditions of unsteadiness. The principles of the phase averaging method are then extended to the case of PIV measurements and both theoretical and practical criterions are given. Examples of potential applications of the phase averaging method for quantitative PIV analyses on an airfoil oscillating through dynamic stall and submitted to strong conditions of unsteadiness are also presented.

1
Introduction

Extracting mean and fluctuating parts from instantaneous measurements performed in a turbulent time-varying flow is an old problem appearing in several domains of fluid mechanics and which concerns different classes of natural and forced unsteady flow configurations. For many years, measurements in steady flows were mainly performed with pointwise measurement systems as for instance, pressure or temperature probes, hot-wire anemometry and Laser Doppler Velocimetry (LDV) for velocity measurements. The inherent flow unsteadiness was thus investigated using an averaging method based on the well-known Reynolds decomposition.

Measurements of the velocity field in complex time-dependant flow configurations, as those generated over pitching airfoils, have been more recently performed using advanced laser velocimetry techniques such as Embedded Laser Doppler Velocimetry (ELDV) and Particle Image Velocimetry (PIV): see for instance Berton et al. (1997), Pascazio et al. (1996, 1997), Oshima and Ramaprian (1997), Wernert et al. (1996, 1997) and Wernert (1997). Hence, the trend is now not only to obtain a few instantaneous velocity data corresponding to some characteristic phases of the investigated phenomenon, but also to register a large number of quantitative instantaneous velocity fields in order to derive mean and fluctuating parts from them.

Additionally, some recent attemps were made to decompose instantaneous PIV velocity fields into mean and fluctuating parts (Yao and Parshal (1994), Raffel et al. (1996), Vogt et al. (1996) and Ullum et al. (1997)). In these unsteady flow configurations, the velocity flowfield is supposed to be decomposable into organized and turbulent components and a ≪phase≫ or ≪ensemble averaging method≫ is employed. However a critical analysis of these studies reveals that the number N of cycles selected in the decomposition method to extract a correct phase averaged value is generally not considered and this can lead to misleading data and errors in the analysis of the PIV results.

In the present work, an attempt is made to address some of the points previously raised. The periodic flow configurations generated over a NACA 0012 pitching airfoil are investigated for different conditions of unsteadiness producing either a transition/laminarisation process of the boundary-layer or a separation/reattachment process of the flow on the airfoil upper side. In both cases the order of procedure to theoretically determine the number N of cycles required to perform a correct phase averaged decomposition is discussed and a practical criterion is proposed. The use of such a criterion is first illustrated in the case of ELDV measurements across the transitional boundary-layer at moderate conditions of unsteadiness. The principles of the phase averaging method are then extended to the case of PIV measurements and both theoretical and practical criterions are given. Examples of potential applications for quantitative PIV analyses on an airfoil oscillating through dynamic stall and submitted to strong conditions of unsteadiness are also presented.

2
Principles of the phase averaging method

In the case of periodic unsteady flows, several methods have been proposed to decompose a measured time-varying signal $u(t)$ into a mean part and a fluctuating part: for example, phase averaging (with or without windows) obtained by conditional

Received: *8 April 1998*/*Accepted*: *6 November 1998*

P. Wernert
French-German Research Institute of Saint-Louis (ISL)
5, rue du Général Cassagnou
F - 68300 Saint-Louis, France

D. Favier
Université de la Méditérranée, CNRS UMR 6594
Institut de Recherche sur les Phénomènes Hors-Equilibre (IRPHE)
Laboratoire ASI, Parc Scientifique de Luminy
163, avenue de Luminy, Case 918
F - 13288 Marseille, France

Correspondence to: P. Wernert

sampling, frequency filtering, cycle-by-cycle smoothing (Tiedermann et al. 1988; Enotiadis et al. 1990). Probably the most widely used is the phase averaging method for which the measured time-varying signal $u(t)$ for the given measurement point is written as

$$u(t)=\langle u(t)\rangle+u'(t) \tag{1}$$

where

$$\langle u(t)\rangle=\lim_{N\to\infty}\frac{1}{N}\sum_{i=1}^{N}u(t+(i-1)T) \tag{2}$$

is the phase average or ensemble average term,

$$u'(t)=u(t)-\langle u(t)\rangle \tag{3}$$

the fluctuations term and T, the period of the cyclic flow. In practice, the phase average velocity has to be determined using (2) over a finite number N of cycles, and the corresponding estimation of $\langle u(t)\rangle$ is thus obtained as

$$\langle u(t,N)\rangle_{\text{est}}=\frac{1}{N}\sum_{i=1}^{N}u(t+(i-1)T) \tag{4}$$

Based on this formulation, it appears that for N sufficiently large, we can expect to have

$$|\langle u(t,N)\rangle_{\text{est}}-\langle u(t)\rangle|<\varepsilon \tag{5}$$

where ε has an arbitrary small positive value: the estimation $\langle u(t,N)\rangle_{\text{est}}$ is then converging towards the true phase average $\langle u(t)\rangle$. As the estimation of $\langle u(t)\rangle$ depends strongly on N, it appears that the choice of the number N of cycles to be used in the averaging process is the critical point of the phase averaging method. However, in almost all experiments, this number N is only determined by the amount of data which can be stored on the computer hard disk system (a typical value for N is a few hundred). Actually, in order to derive correct phase average and fluctuating parts, N should be properly determined so as to satisfy the condition of Eq. (5). It is worthy to note that N is not a constant but is a function of both the instant t and the location of the considered measurement point. In practice however (LDV measurements for example), N is usually taken as a constant for all instant t, so that N is only a function of the location of the considered measurement point.

3
Practical determination of the number *N* of cycles required for correct phase averaging

The above considerations have shown that the correct use of the phase average method is in turn a problem of estimation. The general theory of estimation indicates that a "good" estimator must have following properties: no bias, efficiency and consistency (Martin 1971). Another related approach is to use confidence intervals (Bowker and Lieberman 1965). It is not the purpose here to discuss the use of the phase averaging method from these points of view. Instead of that, we are merely looking for a practical and simple criterion which is useful for determining the number N of cycles required for a correct use of the phase averaging method. It is then straightforward to see that the convergence condition of Eq. (5) is of no practical use since $\langle u(t)\rangle$ cannot be measured. Therefore, the condition of Eq. (5) must be replaced by another one. If N_{max} denotes the maximum number of cycles being recorded during the measurements, a simple and practical condition would be, for example:

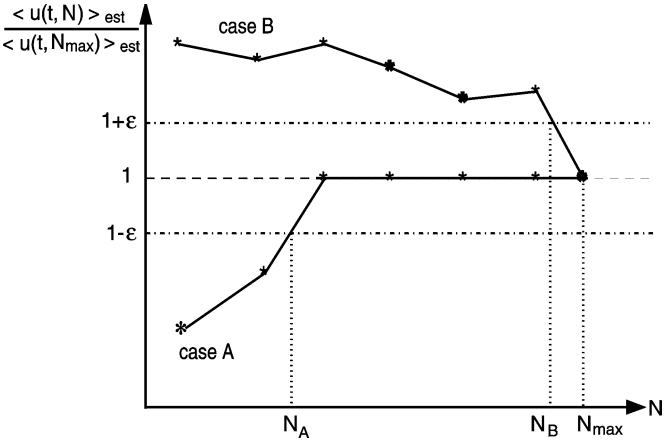

Fig. 1. Practical condition for convergence of the $\langle u(t,N)\rangle_{\text{est}}$ series

$$|\langle u(t,N)\rangle_{\text{est}}-\langle u(t,N_{\max})\rangle_{\text{est}}|\langle\varepsilon|\langle u(t,N_{\max})\rangle_{\text{est}}| \tag{6}$$

which can then be rewritten as

$$1-\varepsilon<\frac{\langle u(t,N)\rangle_{\text{est}}}{\langle u(t,N_{\max})\rangle_{\text{est}}}<1+\varepsilon \tag{7}$$

It should be noticed that the condition of Eq. (7) is always fulfilled for $N=N_{\max}$. Hence, two different cases can appear as shown in Fig. 1. In case A, Eq. (7) is fulfilled for a number of cycles $N=N_A\ll N_{\max}$ which indicates that N_A cycles are enough to ensure convergence of the $\langle u(t,N)\rangle_{\text{est}}$ series. In case B, Eq. (7) is fulfilled for $N=N_B$ with N_B very close to $N_{\max}$ and this shows that the number $N_{\max}$ of cycles being recorded is not sufficient for a correct estimation of $\langle u(t)\rangle$. Examples of the use of Eq. (7) will be given in the next section.

4
ELDV measurements on a pitching airfoil and use of the phase averaging method

To the authors knowledge, no systematic measurements have so far been undertaken for determining the optimal number of cycles required to derive a correct mean flow/fluctuating flow decomposition by means of a phase averaging process. Hence, this problem has been recently investigated at the IRPHE/ASI Laboratory[1] using Embedded Laser Doppler Velocimetry (ELDV) which is suited for unsteady flow measurements above a moving surface (Favier et al. 1996; Pascazio et al. 1996, 1997; Berton et al. 1997).

As an example, Figs. 2 and 3 show the phase average of the longitudinal and normal velocity components $\langle u\rangle$ and $\langle v\rangle$ which have been determined (Pascazio et al. 1996; Favier et al. 1996) using the ELDV technique along the normal distance y to the wall (0.5 mm $\leqslant y\leqslant$ 100 mm), located at the longitudinal abscissa s on the upper side of a NACA 0012 airfoil (chord $c=30$ cm and $s/c=0.67$) oscillating in pitch in the following

[1] Laboratoire d'Aérodynamique Subsonique Instationnaire de l'Institut de Recherche sur les Phénomènes Hors-Equilibre

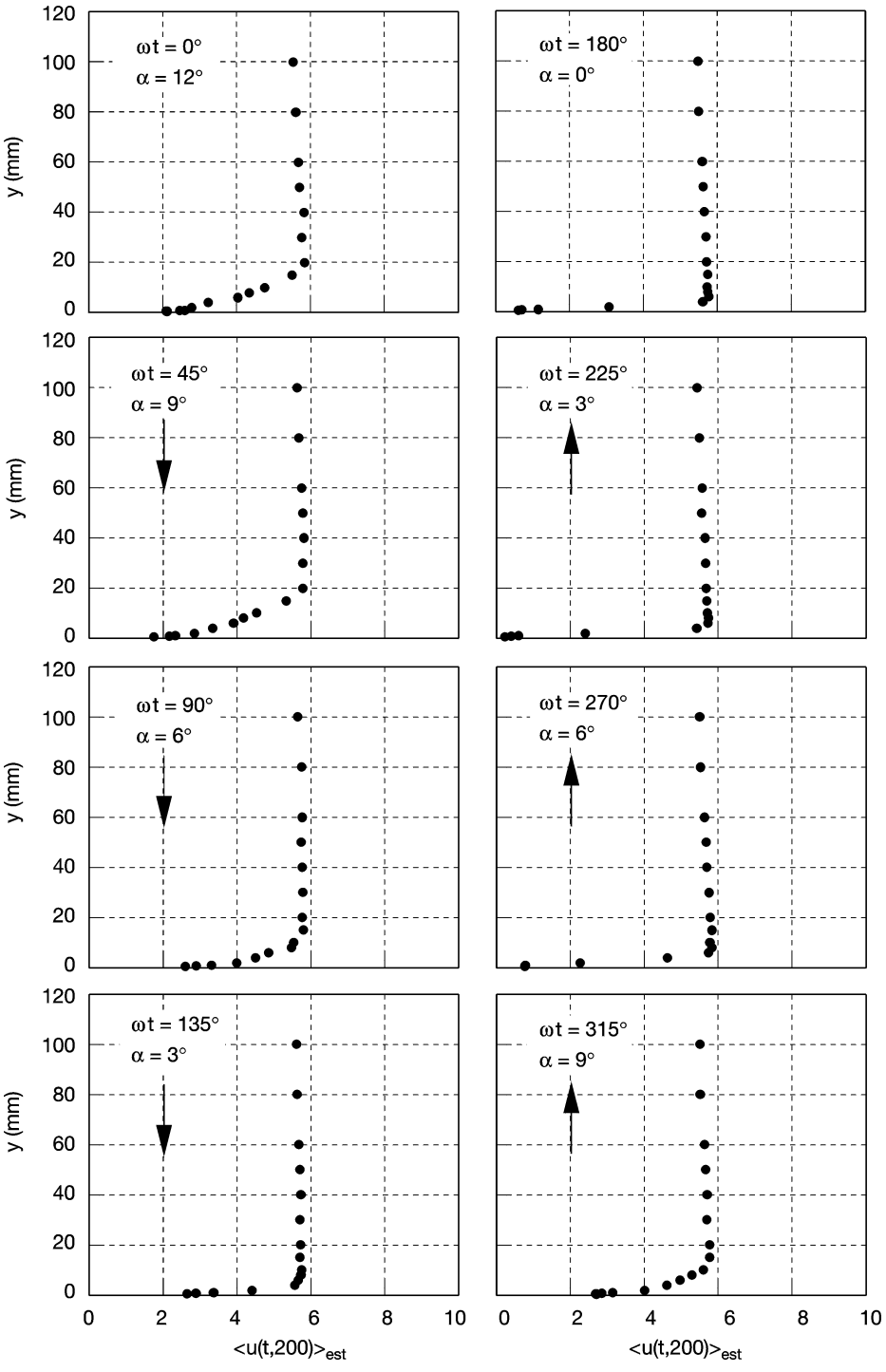

Fig. 2. Phase average $\langle u(t,200)\rangle_{\text{est}}$ longitudinal velocity component on a NACA0012 airfoil oscillating in pitch: $\alpha_0 = 6^\circ$; $\Delta\alpha = 6^\circ$; $k = 0.188$; $Re = 10^5$; $s/c = 0.67$

conditions: freestream velocity $U_\infty = 5$ m/s, airfoil incidence variations $\alpha(t) = \alpha_0 + \Delta\alpha \cos(\omega t)$, mean incidence $\alpha_0 = 6^\circ$, incidence amplitude $\Delta\alpha = 6^\circ$ and reduced frequency $k = \omega c/2U_\infty = 0.188$.

For such oscillating conditions which correspond to moderate conditions of unsteadiness, the period T of the pitching motion has been divided into 256 phases ωt (with $0^\circ \leqslant \omega t \leqslant 360^\circ$) and data acquisitions have been accumulated over successive cycles at each phase ωt of the period, until a total amount of $N_{\max} = 300$ velocity samples per phase was obtained on each component. At each altitude y above the wall, Eq. (4) has been used to get the estimation of the phase average velocity components $\langle u(t,N)\rangle_{\text{est}}$ and $\langle v(t,N)\rangle_{\text{est}}$, where the number of cycles N has been selected at 8 different values within the range $10 \leqslant N \leqslant 300$. In Figs. 2 and 3, the result of this phase averaging process is examplified for the specific value of $N = 200$: the $\langle u(t,200)\rangle_{\text{est}}$ and $\langle v(t,200)\rangle_{\text{est}}$ velocity profiles are plotted as a function of the altitude y normal to the wall ($0.5 \text{ mm} \leqslant y \leqslant 100$ mm) at 8 different values of the phase ωt along the period. At such an abscissa $s/c = 0.67$ on the upper side of the airfoil, the $\langle u(t,200)\rangle_{\text{est}}$ and $\langle v(t,200)\rangle_{\text{est}}$ profiles exhibit a typical process of transition/laminarisation of the boundary-layer along the period as shown by Pascazio et al. (1997) and Berton et al. (1997).

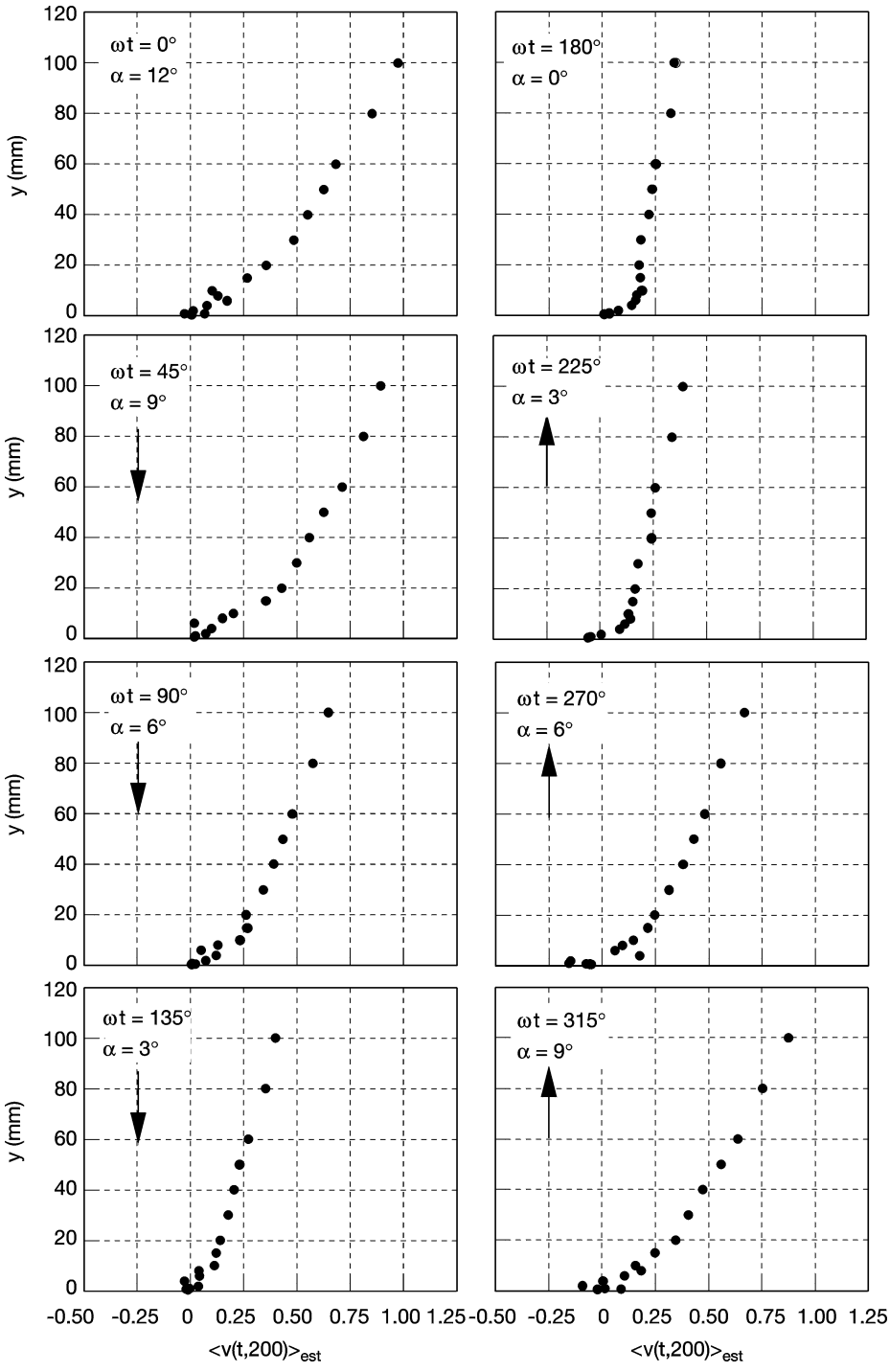

Fig. 3. Phase average $\langle v(t,200)\rangle_{\text{est}}$ normal velocity component on a NACA0012 airfoil oscillating in pitch: (same oscillating conditions as in Fig. 2)

Some evidences of this unsteady boundary-layer behaviour are given in Fig. 4 where the non dimensionalized velocity component $\langle u(t,200)\rangle_{\text{est}}/U_e$ is plotted as a function of η ($\eta = y\sqrt{Re_s}/s$) at 8 different values of the phase ωt. In this figure, Re_s represents the local Reynolds number based on the curvilinear abscissa s from the leading edge ($Re_s = sU_\infty/\nu$) and U_e is the local longitudinal velocity component at the edge of the boundary-layer. These experimental profiles obtained with $N = 200$ are compared to both laminar and turbulent theoretical profiles deduced respectively from the Polhausen approximation and from the turbulent power law (1/4th). As a function of ωt, the laminar boundary-layer regime is thus shown to occur at low values of the instantaneous incidence ($160^\circ \leqslant \omega t \leqslant 260^\circ$), while the transitional regime to turbulence occurs for $270^\circ \leqslant \omega t \leqslant 360^\circ$ and the laminarisation process for $135^\circ \leqslant \omega t \leqslant 160^\circ$. More details on the occurrence of the transition/relaminarisation process can be found in Pascazio et al. (1996) and Favier et al. (1996).

The influence of varying the value of N in the phase averaging process is then shown on Figs. 5 and 6 for similar pitching conditions as in Figs. 2 to 4. In Figs. 5 and 6, the phase average velocities $\langle u(t,N)\rangle_{\text{est}}$ and $\langle v(t,N)\rangle_{\text{est}}$ are plotted as a function of ωt at 3 different altitudes y above the airfoil wall corresponding to the inner region of the boundary-layer

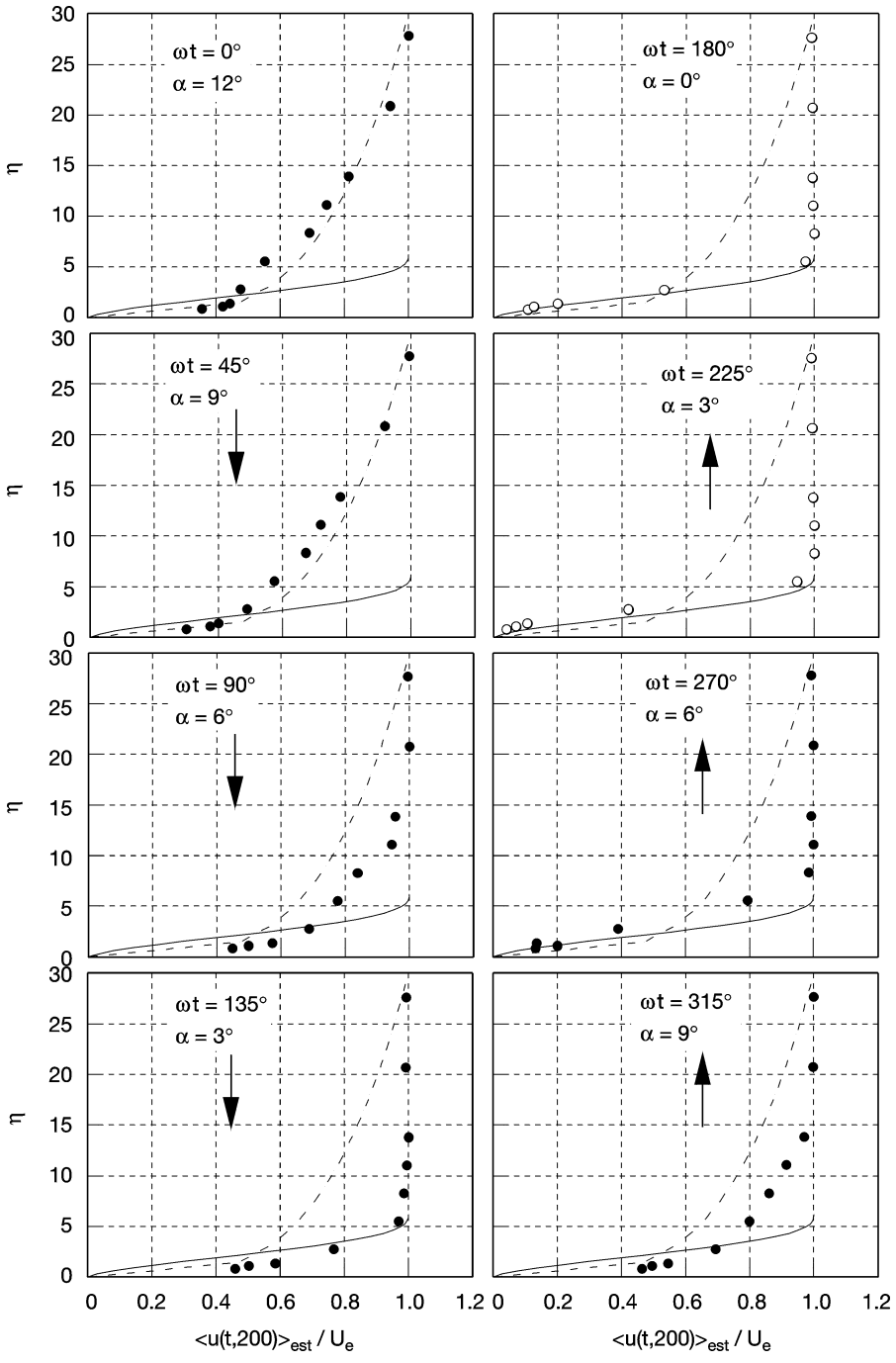

Fig. 4. Phase average $\langle u(t,200)\rangle_{\text{est}}/U_e$ as a function of η (same oscillating conditions as in Fig. 2): Theoretical profiles: —— laminar; – – – – turbulent Experimental profiles; ○ laminar; ● turbulent

($y=0.8$ mm), the edge of the boundary-layer ($y=2$ mm) and the potential flow outside the boundary-layer ($y=10$ mm). At each altitude y, the $\langle u(t,N)\rangle_{\text{est}}$ and $\langle v(t,N)\rangle_{\text{est}}$ velocity profiles are plotted for 5 different values of N within the range $10\leqslant N\leqslant 200$. For clarity of the plots, only 64 different values of ωt are shown (256 values were recorded for each y and each N). The effect of increasing the number of cycles N is shown to be small in the potential flow region ($y=10$ mm), at least on the $\langle u(t,N)\rangle_{\text{est}}$ component and for phases $135^\circ\leqslant\omega t\leqslant 270^\circ$ corresponding to the lower instantaneous incidences of the airfoil. At the edge of the boundary-layer ($y=2$ mm), the dependence on N of the phase average values of both $\langle u(t,N)\rangle_{\text{est}}$ and $\langle v(t,N)\rangle_{\text{est}}$ is shown to be more accentuated, specially during the transitional regime ($\omega t\geqslant 270^\circ$) and the turbulent regime ($\omega t\leqslant 160^\circ$). While close to the wall ($y=0.8$ mm), the $\langle u(t,N)\rangle_{\text{est}}$ and $\langle v(t,N)\rangle_{\text{est}}$ profiles are shown to be strongly dependent on the value of N at all phases ωt of the period. It is also seen on these figures that the $\langle v(t,N)\rangle_{\text{est}}$ profiles are generally much more sensitive to N than the $\langle u(t,N)\rangle_{\text{est}}$ profiles.

In order to identify, for such moderate unsteady flow conditions, which values of N are sufficiently high to fullfill the practical condition of Eq. (7) and thus to render the above described phase averaging process independent of the number of cycles, Figs. 7 and 8 show the evolution of the non dimensionalized $\langle u(t,N)\rangle_{\text{est}}/\langle u(t,300)\rangle_{\text{est}}$ and $\langle v(t,N)\rangle_{\text{est}}/$

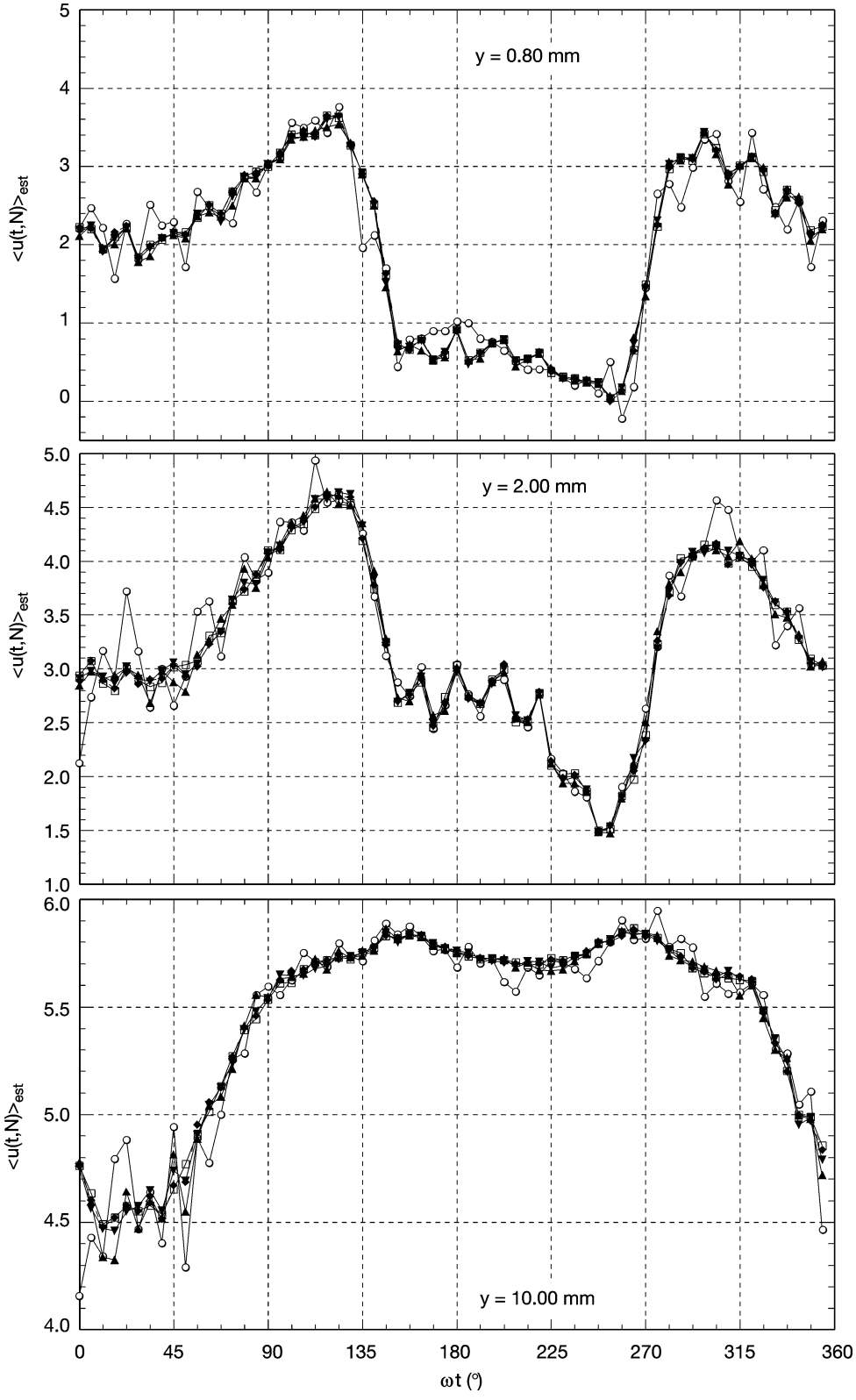

Fig. 5. $\langle u(t,N)\rangle_{\text{est}}$ velocity component as a function of ωt at three different altitudes y above the airfoil wall (same oscillating conditions as in Fig. 2): —○— $N=10$ cycles; —▲— $N=50$; —▼— $N=100$; —◆— $N=150$; —□— $N=200$

$\langle v(t,300)\rangle_{\text{est}}$ velocity components at a given altitude $y=$ constant and as a function of N varying from $N=10$ to $N_{\max}=300$ cycles. The boundaries corresponding to the thresholds $(1-\varepsilon)$ and $(1+\varepsilon)$ of Eq. (7) with $\varepsilon=0.03$ are plotted in dotted lines. The Fig. 7 clearly indicates, at the four selected values of the phase $\omega t=45^\circ$, 135°, 180° and 270°, that the convergence is obtained on the $\langle u(t,N)\rangle_{\text{est}}$ component when the number of cycles is higher than $N=150$ for the three considered values of y. On the other hand, in Fig. 8, a number of cycles $N\geqslant 200$ is shown to be required on the $\langle v(t,N)\rangle_{\text{est}}$ component at the edge ($y=2$ mm) and outside of the boundary-layer ($y=10$ mm), while $N>300$ cycles is required in the inner region of the

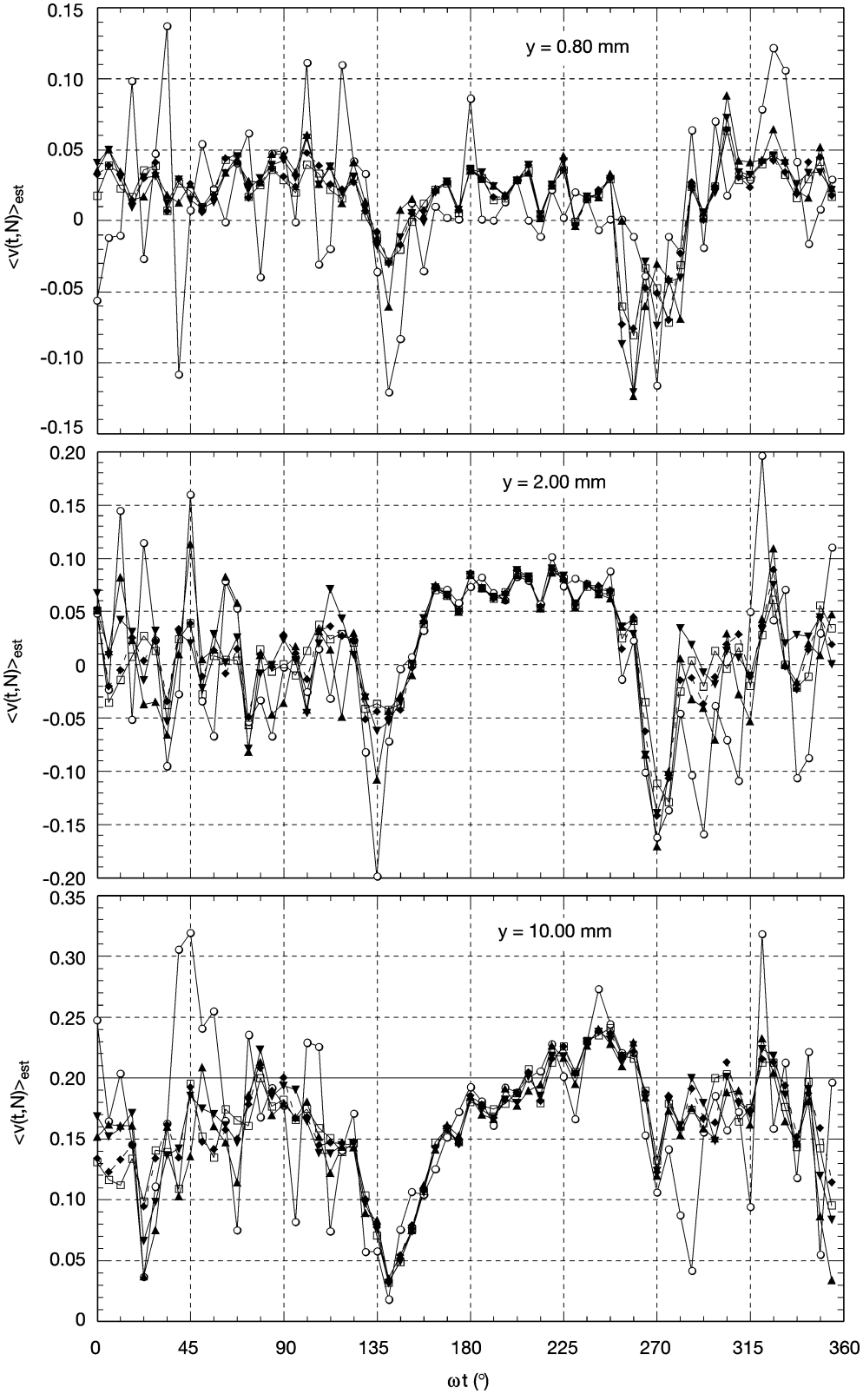

Fig. 6. $\langle v(t,N)\rangle_{est}$ velocity component as a function of ωt at three different altitudes y above the airfoil wall (same oscillating conditions as in Fig. 2): —○— $N=10$ cycles; —▲— $N=50$; —▼— $N=100$; —◆— $N=150$; —□— $N=200$

boundary-layer ($y=0.8$ mm) for $\omega t=45^\circ$ and for the laminarisation flow regime ($\omega t=135^\circ$).

Consequently, for the pitching conditions selected in the present case, it appears that in order to fulfill the criterion of Eq. (7) on both velocity components at each phase ωt and during all the laminar, transitional and turbulent boundary-layer regimes along the period, the number N_{max} of cycles to be considered has to be increased to $N_{max}>300$. It should also be noticed that for oscillating conditions which involve the dynamic stall phenomenon (for instance, $\alpha_0=12^\circ$ and

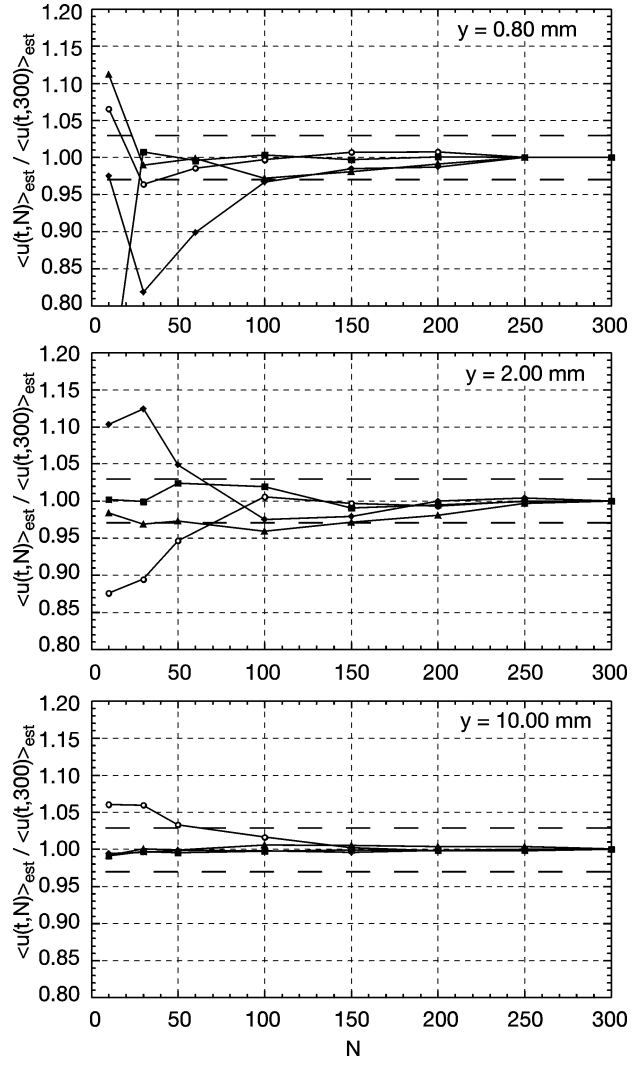

Fig. 7. Evolution of the nondimensionalized $\langle u(t,N)\rangle_{est}/\langle u(t,300)\rangle_{est}$ longitudinal velocity component as a function of N for $N_{max}=300$ cycles. The two horizontal dotted lines correspond to the thresholds $(1-\varepsilon)$ and $(1+\varepsilon)$ of Eq. (7) with $\varepsilon=0.03$ (same oscillating conditions as in Fig. 2): —○— $\omega t=45^\circ$; —■— $\omega t=135^\circ$; —▲— $\omega t=180^\circ$; —◆— $\omega t=270^\circ$

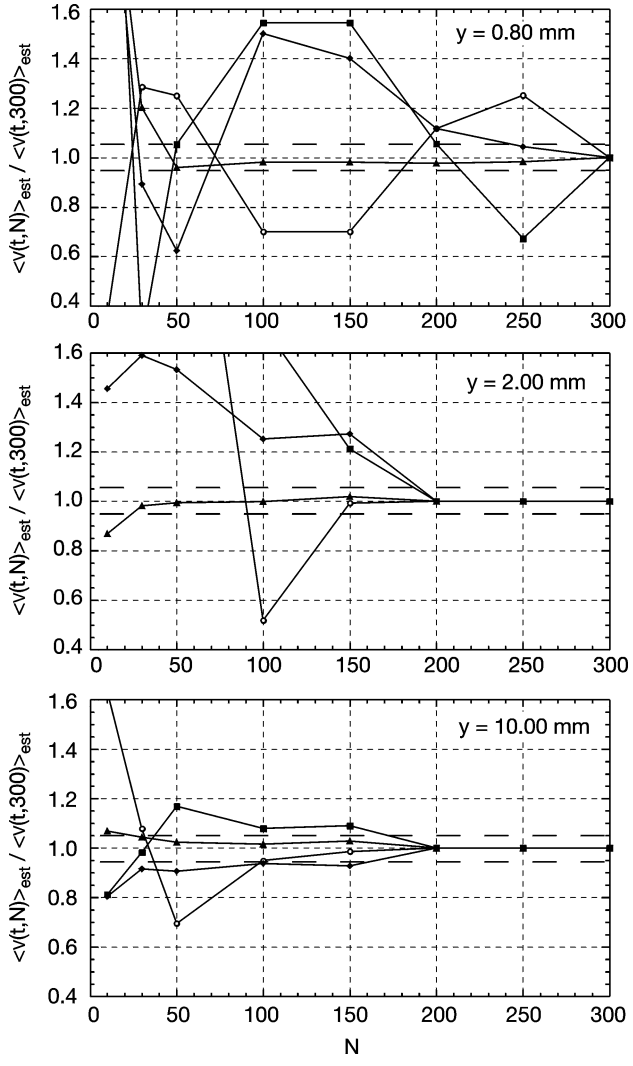

Fig. 8. Evolution of the nondimensionalized $\langle v(t,N)\rangle_{est}/\langle v(t,300)\rangle_{est}$ longitudinal velocity component as a function of N for $N_{max}=300$ cycles. The two horizontal dotted lines correspond to the thresholds $(1-\varepsilon)$ and $(1+\varepsilon)$ of Eq. (7) with $\varepsilon=0.03$ (same oscillating conditions as in Fig. 2): —○— $\omega t=45^\circ$; —■— $\omega t=135^\circ$; —▲— $\omega t=180^\circ$; —◆— $\omega t=270^\circ$

$\Delta\alpha=10^\circ$) and the occurrence of the cyclic separation/reattachment process of the flow on the upper side of the airfoil, the adequate number N needs certainly to be significantly increased to fullfill the criterion of Eq. (7) at each phase of the flow separation and flow reattachment regimes.

5
Phase averaging method in PIV measurements

Particle Image Velocimetry (PIV) is a well-known non-intrusive technique which provides instantaneous two-dimensional velocity fields (components $u(x,y,t)$ and $v(x,y,t)$) at an instant t, with measurement points (x,y) located on a regular grid (Grant (1994)). When applied to unsteady flows executing cycles of period T, the instantaneous PIV velocity fields measured at a given phase of the cycle can be decomposed into mean and fluctuating parts in the same way as mentioned before, i.e. at each measurement point (x,y) and at each measurement time t, the velocity components can be expressed as

$$u(x,y,t)=\langle u(x,y,t)\rangle+u'(x,y,t) \tag{8}$$

and

$$v(x,y,t)=\langle v(x,y,t)\rangle+v'(x,y,t) \tag{9}$$

where $\langle u(x,y,t)\rangle$, $u'(x,y,t)$, $\langle v(x,y,t)\rangle$ and $v'(x,y,t)$ are defined and calculated in a similar way as in Eqs. (1)–(4). In practice, the terms $\langle u(x,y,t)\rangle$ and $\langle v(x,y,t)\rangle$ are calculated over a finite number $N_{x,y}$ of cycles as indicated in Eq. (4). Hence, to assess a correct phase averaging decomposition, the two following conditions must be simultaneously verified at each measurement point (x,y):

$$|\langle u(x,y,t,N_{x,y})\rangle_{est}-\langle u(x,y,t)\rangle|<\varepsilon_1 \tag{10}$$

$$|\langle v(x,y,t,N_{x,y})\rangle_{est}-\langle v(x,y,t)\rangle|<\varepsilon_2 \tag{11}$$

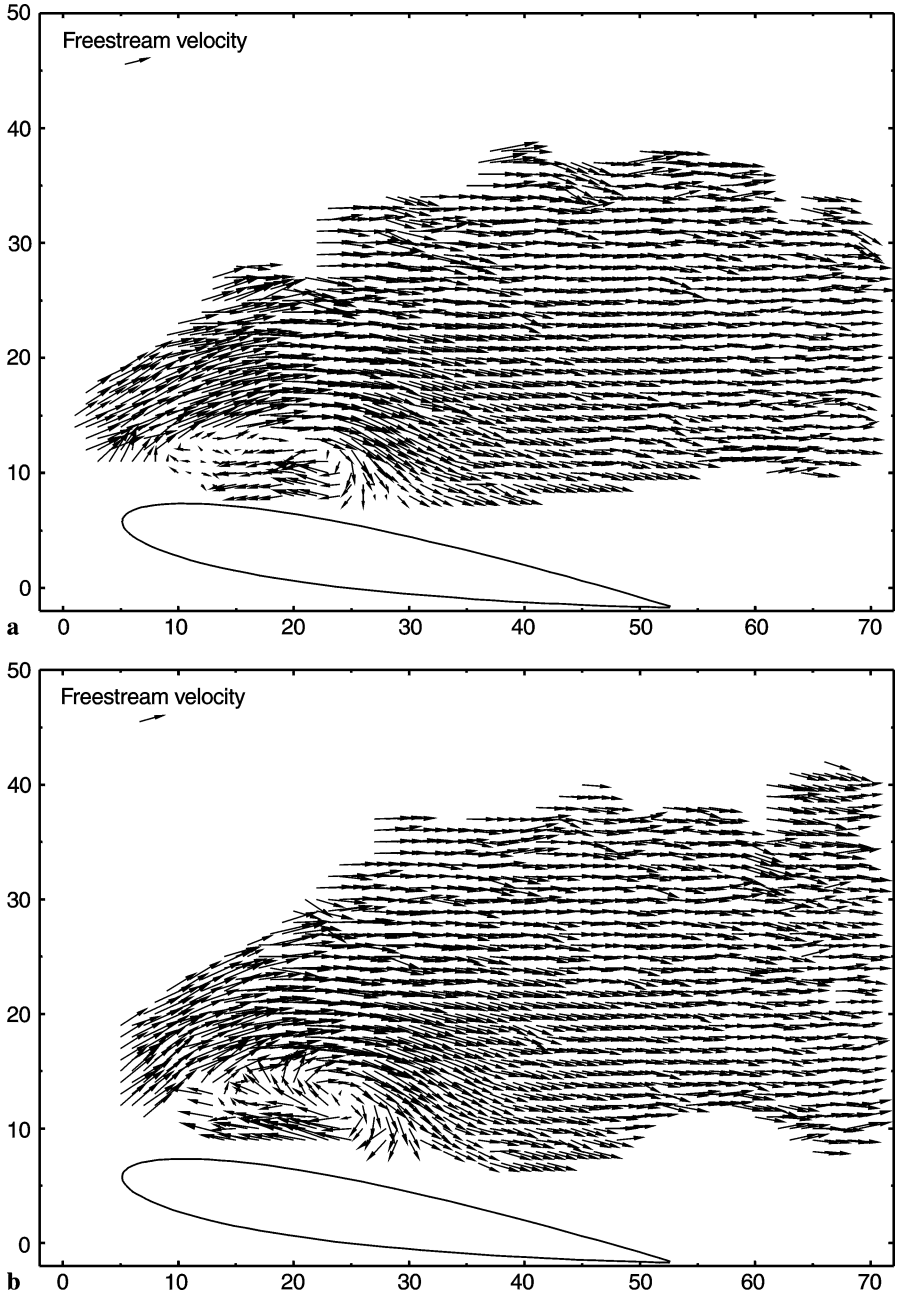

Fig. 9. **a** (top) and **b** (bottom): PIV velocity fields over a pitching NACA 0012 airfoil at the same incidence of 24° upstroke in two different oscillation cycles ($c=20$ cm, $U_\infty=14$ m/s, $\alpha(t)=15^\circ+10^\circ\sin(\omega t)$, $k=0.30$)

where ε_1 and ε_2 have small positive values. In practice, the same criterion as in Eq. (7) will be used, i.e.:

$$1-\varepsilon_1<\frac{\langle u(x,y,t,\ N_{x,y})\rangle_{\text{est}}}{\langle u(x,y,t,\ N_{\max})\rangle_{\text{est}}}<1+\varepsilon_1 \tag{12}$$

$$1-\varepsilon_2<\frac{\langle v(x,y,t,\ N_{x,y})\rangle_{\text{est}}}{\langle v(x,y,t,\ N_{\max})\rangle_{\text{est}}}<1+\varepsilon_2 \tag{13}$$

These conditions lead then to the minimum number $N_{x,y}$ of cycles to be used for each measurement point (x,y). For a complete PIV velocity field, the minimum number N of cycles required is then given by:

$$N=\max(N_{x,y}) \tag{14}$$

This is an important difference when compared to ELDV measurements: indeed, for ELDV measurements, the number N of cycles can be different from one point to the other. In the case of PIV measurements, as the whole velocity field is recorded simultaneously, the number of cycles is obviously the same for all measurement points. As a consequence, N can become a very high number. On another hand, N is now no more a function of the measurement point (x,y), but is only a function of the measurement instant t.

Phase averaging methods have already been employed in PIV measurements and reported in the literature. For instance, Yao and Pashal (1994) made PIV measurements in the wake of a natural laminar airfoil flow and obtained statistics of the flowfield by phase averaging over $N=240$ PIV samples. Raffel et al. (1996) report PIV velocity fields over an helicopter rotor model in a wind-tunnel: three different flow areas are considered and two different numbers of cycles are used: $N=35$ and $N=100$. Vogt et al. (1996) measured the wing tip vortex

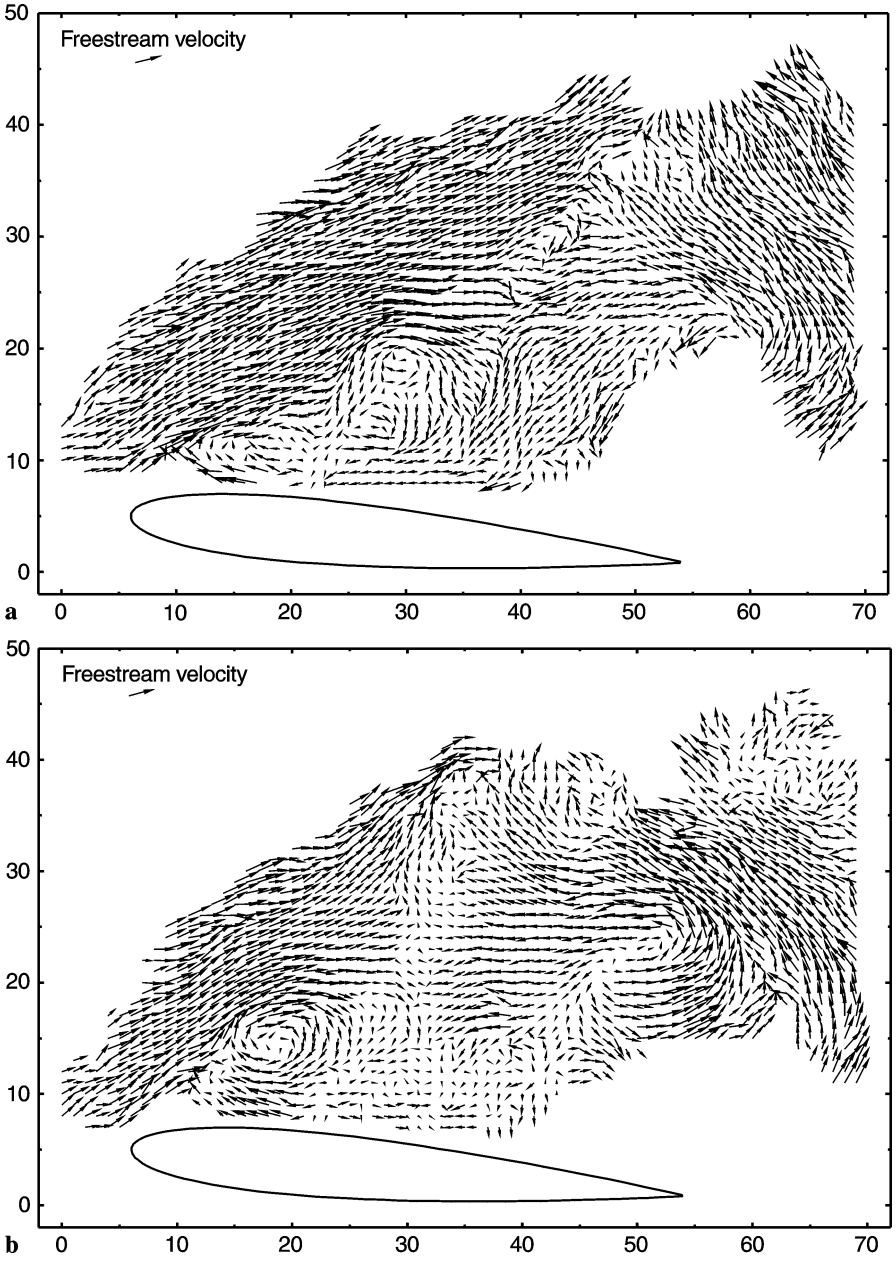

Fig. 10. a (top) and **b** (bottom): PIV velocity fields over a pitching NACA 0012 airfoil at the same incidence of 20° downstroke in two different oscillation cycles ($c = 20$ cm, $U_\infty = 14$ m/s, $\alpha(t) = 15^\circ + 10^\circ \sin(\omega t)$, $k = 0.30$)

over a NACA 0012 airfoil where the PIV velocity fields were averaged over $N = 500$ images. Durget et al. (1997) obtained information about the mean and fluctuating velocity flowfield in a combustion engine by phase averaging over 200 PIV realizations. Finally, Ullum et al. (1997) report on the complex separated flowfield behind a fence by averaging over almost $N = 3000$ PIV velocity fields.

The important point here is that the choice of the number N of cycles used in the averaging process is not sufficiently discussed and generally not justified in the works mentioned above. This remark is actually valid for most experiments using phase averaging methods, not only with the PIV technique, but also when other global or pointwise measurement methods (LDV, hot wires, pressure transducers or balance techniques) are used. As a consequence, it has not been proved that the conditions of Eq. (10) and (11) are fulfilled and so, the decomposition into mean and fluctuating parts may be incorrect in the above mentioned PIV analyses.

PIV experiments have also been made at ISL[2] in order to investigate the complex separated velocity field over a NACA 0012 airfoil pitching under deep dynamic stall conditions (due to strong conditions of unsteadiness: $\alpha_0 = 10^\circ$, $\Delta\alpha = 15^\circ$ and $k = 0.30$) in an incompressible flow (Raffel et al. 1995; Wernert et al. 1996, 1997; Wernert 1997). The results have revealed that the velocity field can be considered as reproducible from cycle to cycle during the phase of increasing airfoil incidences (Figs. 9a and b). But during the phase of decreasing airfoil incidences, after the complete separation of the flowfield from

[2]French-German Research Institute of Saint-Louis

the airfoil upper side, the PIV velocity fields clearly exhibit a non-reproducible effect, i.e. for the same instantaneous airfoil incidence, the measured vortex structures do not have the same spatial characteristics (location, size) from cycle to cycle (Figs. 10a and b). More details can be found in Wernert et al. (1997) and Wernert (1997). The number of registered PIV velocity fields was here too low to undertake a decomposition by phase averaging. Although the number N of required cycles should be very high according to Eq. (14), new PIV measurements would indeed show if the deep dynamic stall phenomenon can, during the phase of decreasing incidences, be reduced to a mean and a fluctuating parts. In this case, the cycle to cycle variations observed on the vortex structures of Figs. 10a and b can be considered as spatial fluctuations around a mean flow. If such a reduction cannot be reached, a new approach to the dynamic stall problem (like that proposed by Truong (1993) based on Hopf bifurcations) should be considered.

6 Conclusions

From the present investigation conducted on unsteady flow configurations generated over periodic pitching airfoils, it should be concluded on the following recommendations. When the phase averaging method is used in LDV measurements, the required number N of cycles must satisfy the theoretical condition of Eq. (5) and a practical condition is given by Eq. (7). When the phase averaging method is used in PIV measurements, it is required to average over a number N of cycles in order to fullfill the conditions of Eqs. (10) and (11) at each point of the velocity field. A practical local condition is then Eqs. (12) and (13) which leads to the overall condition of Eq. (14). Potential users of this method should also be aware of the fact that this optimal number N can become very high in PIV, especially if measurements are to be performed either in separated or boundary-layer flows or at high values of the flow unsteadiness parameters. If the number N of required cycles is too high for the capabilities of the experimental set-up or PIV measurement system, alternative methods must be employed like those mentioned either by Tiedermann et al. (1988) and Enotiadis et al. (1990) or by Brereton and Kodal (1992, 1994).

Finally, it should be underlined that the simple phase averaging method discussed here is based on the assumption that the period T of the flow is known and constant in time. If T is unknown or not constant in time, other phase averaging methods with more complex conditional sampling techniques like the variable-interval time averaging algorithm (VITA, see Morrison et al. (1989)) may be used.

References

Berton E; Favier D; Maresca C (1997) Embedded L.V. methodology for boundary-layer measurements on oscillating models. AIAA Paper 97-1832

Bowker AH; Lieberman GJ (1965) Méthodes statistiques de l'ingénieur. Editions Dunod.

Brereton GJ; Kodal A (1992) A frequency-domain filtering technique for triple decomposition of unsteady turbulent flow. J Fluids Engng 114: 45–51

Brereton GJ; Kodal A (1994) An adaptative turbulence filter for decomposition of organized turbulent flows. Phys Fluids 6: 1775–1786

Durget M; Murat M; Guibert P (1997) Caractérisation des champs de concentrations et de l'aérodynamique par tomographie laser dans un cylindre de moteur alternatif. 7ème Colloque National de Visualisation et de traitement d'images en Mécanique des Fluides, Saint-Louis, France: 133–138

Enotiadis AC; Vafidis C; Whitelaw JH (1990) Interpretation of cyclic flow variations in motored internal combustion engines. Exp Fluids 10: 77–86

Favier D; Maresca C; Berton E; Agnes A (1996) Etude expérimentale et numérique du développement de la couche limite instationnaire sur modèles oscillants en écoulement 2D/3D. Rapport de synthèse, Convention DRET 95-052

Grant I (ed) (1994) Selected papers on Particle Image Velocimetry. SPIE Milestone Series, Volume MS 99

Martin BR (1971) Statistics for Physicists. pp. 72–74. London: Academic Press

Morrison JF; Tsai HM; Bradshaw P (1989) Conditional-sampling schemes for turbulent flow based on the variable-interval time averaging (VITA) algorithm. Exp Fluids 7: 173–189

Oshima H; Ramaprian BR (1997) Velocity measurements over a pitching airfoil. AIAA J 35, 1: 119–126

Pascazio M; Autric JM; Favier D; Maresca C (1996) Unsteady boundary-layer measurement on oscillating airfoils: transition and separation phenomena in pitching motion. AIAA Paper 96-0035

Pascazio M; Autric JM; Favier D; Maresca C (1997) Boundary-layer characterization on moving walls by an embedded laser velocimetry technique. AIAA J 35: 207–209

Raffel M; Kompenhans J; Wernert P (1995) Investigation of the unsteady flow velocity field above an airfoil pitching under deep dynamic stall conditions. Exp Fluids 19: 103–111

Raffel M; Seelhorst U; Willert C; Vollmers H; Bütefisch KA; Kompenhans J (1996) Measurements of vortical structures on a helicopter rotor model in a wind tunnel by LDV and PIV. 8th International Symposium on Applications of Laser Techniques to Fluid Mechanics, Lisbon, Portugal: 14.3.1–14.3.6

Tiedermann WG; Privette RM; Phillips WM (1988) Cycle-to-cycle variations effects on turbulent shear stress measurements in pulsatile flows. Exp Fluids 6: 265–272

Truong VK (1993) A 2-D Dynamic stall model based on a Hopf bifurcation. 19th Rotorcraft European Forum, Cernobbio, Italie: C23.1–C23.14

Ullum U; Schmidt JJ; Larsen PS; McCluskey DR (1997) Temporal evolution of the perturbed and unperturbed flow behind a fence: PIV analysis and comparison with LDA data. 7th International Conference on Laser Anemometry and Applications, Karlsruhe, Germany: 809–816

Vogt A; Baumann P; Gharib M; Kompenhans J (1996) Investigations of a wing tip vortex in air by means of DPIV. AIAA Paper 96-2254

Wernert P; Geissler W; Raffel M; Kompenhans J (1996) Experimental and numerical investigations of dynamic stall on a pitching airfoil. AIAA J 34: 982–989

Wernert P; Koerber G; Wietrich F; Raffel M; Kompenhans J (1997) Demonstration by PIV of the non-reproducibility of the flow field around an airfoil pitching under deep dynamic stall conditions and consequences thereof. Aerospace, Science and Technology, 1: 125–135

Wernert P (1997) Méthodes de visualisation et de PIV appliquées à l'étude du décrochage dynamique profond et comparaison avec des résultats de simulation numérique. Thesis, Université de la Méditerranée, Marseille, France and ISL-Report R 125/97

Yao C; Pashal K (1994) PIV measurements of airfoil wake-flow turbulence statistics and turbulent structures. AIAA Paper 94-0085